Respiratory Medicine 109 (2015) 1235–1243

Contents lists available at ScienceDirect

Respiratory Medicine

journal homepage: www.elsevier.com/locate/rmed

Review article

Focal pleural tumorlike conditions: Nodules and masses beyond mesotheliomas and metastasis

Maria Clara Fernandes de Paula [a, 1], Dante Luiz Escuissato [b, 2], Luciana Camara Belém [a, 3], Gláucia Zanetti [a, 4], Arthur Soares Souza Jr. [c, 5], Bruno Hochhegger [d, 6], Luiz Felipe Nobre [e, 7], Edson Marchiori [a, *]

[a] Federal University of Rio de Janeiro, Rio de Janeiro, Brazil
[b] Federal University of Paraná, Curitiba, Brazil
[c] Medical School of Rio Preto and Ultra X, São José do Rio Preto, SP, Brazil
[d] Santa Casa de Porto Alegre, Porto Alegre, Rio Grande do Sul, Brazil
[e] Santa Catarina Federal University, Florianópolis, Brazil

ARTICLE INFO

Article history:
Received 23 January 2015
Received in revised form
7 May 2015
Accepted 8 June 2015
Available online 12 June 2015

Keywords:
Pleural diseases
Computed tomography
Tumorlike conditions
Pleural endometriosis
Pleural esplenosis

ABSTRACT

A tumorlike condition of the pleura is any nonmalignant lesion of the pleura or within the pleural space that could be confused with a pleural tumor on initial imaging. Tumorlike conditions of the pleura are relatively rare compared with neoplastic lesions such as mesotheliomas and metastases. Imaging-based diagnosis of these conditions can be difficult due to the similarity of appearance. Thus, recognition of certain imaging patterns and interpretation of these patterns in the clinical context are important. Pleural endometriosis, thoracic splenosis, thoracolithiasis, foreign bodies, pleural pseudotumors and pleural plaques are significant examples of focal tumorlike conditions discussed in this article. Computed tomography is the mainstay imaging technique for the primary assessment of pleural disease, but other imaging methods, such as magnetic resonance imaging and positron-emission tomography, can be of great support in the diagnosis.

1. Introduction

Primary or metastatic tumors and tumorlike conditions may involve the pleura. Imaging plays an important role in the evaluation of pleural disease. Chest radiographs are useful for initial assessment, but findings may not allow confident differentiation of benign from malignant conditions. Computed tomography (CT) is the mainstay imaging technique for primary assessment of pleural disease and affords improved sensitivity for identification of a malignant pleural process. Magnetic resonance imaging (MRI) and positron-emission tomography are complementary techniques that can provide additional staging and prognostic information [1].

Pleural nodules and masses can be divided into tumoral lesions and tumorlike conditions. True tumoral lesions are classified as metastatic or primary, the latter of which can be malignant or benign. The most common pleural tumor is metastatic cancer, and the most common primary pleural tumor is mesothelioma [2,3].

A tumorlike condition is any nonneoplastic lesion of the pleura or within the pleural space that resembles a tumor. These lesions may be classified as focal or diffuse. Focal tumorlike conditions

* Corresponding author. Rua Thomaz Cameron, 438, Valparaiso, CEP 25685.120, Petrópolis, Rio de Janeiro, Brazil.
E-mail addresses: mariaclara_depaula@hotmail.com (M.C. Fernandes de Paula), dante.escuissato@gmail.com (D.L. Escuissato), lubelem@globo.com (L.C. Belém), glauciazanetti@gmail.com (G. Zanetti), asouzajr@gmail.com (A.S. Souza), brunohochhegger@gmail.com (B. Hochhegger), luizfelipenobresc@gmail.com (L.F. Nobre), edmarchiori@gmail.com (E. Marchiori).
[1] Avenida Atlântica, 3806 Apto 612, Copacabana, CEP: 22070-000, Rio de Janeiro, Brazil.
[2] R. General Carneiro, 181, CEP 80060-900, Curitiba, Paraná, Brazil.
[3] Avenida Ayrton Senna, 111 Apto 405, Barra da Tijuca, CEP 22793-000, Rio de Janeiro, Brazil.
[4] Rua Coronel Veiga, 733/504, Centro, CEP 25655-504, Petrópolis, Rio de Janeiro, Brazil.
[5] Rua Cila 3033, CEP 15015-800, São José do Rio Preto, Brazil.
[6] Rua João Alfredo, 558/301, CEP 90050-230, Porto Alegre, Brazil.
[7] R. Desemb. Pedro Silva, 2800, Ap.303B, Coqueiros, CEP 88080-701, Florianópolis, Santa Catarina, Brazil.

http://dx.doi.org/10.1016/j.rmed.2015.06.004
0954-6111/

include thoracic splenosis, pleural endometriosis, thoracolithiasis, foreign bodies, pleural plaques, and pleural pseudotumor [3]. As the imaging characteristics of these conditions can be similar, clinical history and presentation have important roles in differential diagnosis and can help to distinguish the etiology of pleural nodules [1–3].

The purpose of this article is to review the clinical, radiologic, and pathologic findings of focal pleural tumorlike conditions, such as pleural endometriosis, thoracic splenosis, thoracolithiasis, foreign bodies, pleural plaques, and pleural pseudotumor.

2. Pleural endometriosis

Endometriosis is characterized by the growth of endometrium outside the uterine cavity or myometrium. The pelvis and, less frequently, the abdominal cavity are the sites most frequently involved, but endometriosis has been reported in virtually all body compartments [4]. The thoracic cavity is the most frequent extra-abdominopelvic site of endometriosis [5].

Thoracic endometriosis syndrome (TES) is a rare disorder characterized by the presence of functioning endometrial tissue in the pleura, lung parenchyma, or airway [6]. The pathogenesis of this syndrome is not completely understood, and three different theories have been proposed: celomic metaplasia, lymphatic or hematogenous embolization from the uterus or pelvis, and retrograde menstruation with subsequent transperitoneal–transdiaphragmatic migration of endometrial tissue [7,8].

TES includes five well-recognized clinical entities, divided into pleural and pulmonary forms. The pleural form includes catamenial pneumothorax (CP), non-catamenial endometriosis-related pneumothorax, and catamenial hemothorax. The pulmonary form includes catamenial hemoptysis and lung nodules [9]. Affected patients frequently have a history of infertility, severe endometriosis, and recurrent spontaneous pneumothoraces, occurring between 24 h before and 72 h after the onset of menses [10]. The right hemithorax is involved in more than 90% of all forms [5].

A definitive diagnosis of thoracic endometriosis requires histologic confirmation. In certain cases, a presumptive diagnosis can be made based on clinical history and a positive response to appropriate treatment [11]. Invasive methods for the diagnosis of thoracic endometriosis include video-assisted thoracoscopy with biopsy [7]. If possible, this examination should be timed around the beginning of the menstrual flow to allow maximum visibility of potential endometriotic implants [12].

In patients with pleural endometriosis, chest X-rays may reveal pleural effusion, pneumothorax, or pleural nodules, but they are often normal [6]. Sonography of the upper abdomen and chest may show defects in the hemidiaphragm, as well as mixed echogenic materials of endometrial tissue in the pleural space [13].

Although the CT findings of TES are poorly specific, CT remains the first-line imaging method, as it can be used to rule out other diagnoses and map lesions for surgery [9,14]. CT examination during menses is more sensitive, as lesions may vary in size or disappear during other phases of the menstrual cycle [15,16]. CT images can show pneumothorax or hydropneumothorax [17] (Fig. 1), and may also demonstrate nodular lesions that change in appearance during the menstrual cycle [15,18]. Pleural implants appear as hypoattenuating areas on CT, sometimes associated with an isoattenuated component, depending on size and blood content [9]. The pattern will vary depending on the size of the implant, but enhancement is characteristic [9].

MRI is expected to have a prominent role in the examination of patients with CP because it provides better spatial resolution, contrast, and ability to characterize hemorrhagic tissues. MRI is said to be more accurate than CT in the detection of CP [17,19–22].

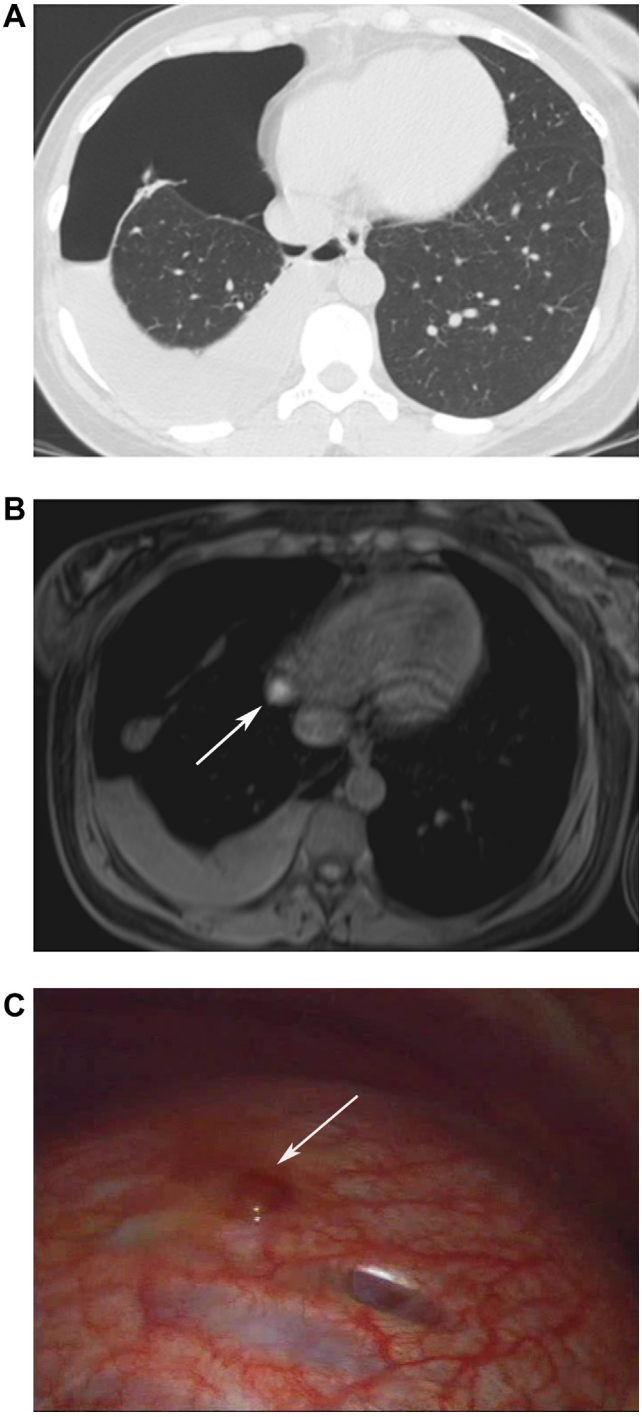

Fig. 1. A 35-year-old woman with pleural endometriosis. The patient presented with chest pain and dyspnea occurring monthly, coincident with menses. A. Computed tomography at the level of the lower lobes of the lungs shows a right hydropneumothorax. B. Axial T1-weighted magnetic resonance image reveals an oval, well-defined pleural lesion with intermediate signal intensity (arrow) and hydropneumothorax. Pleural effusion also shows intermediate signal intensity, probably due to the blood component of fluid. C. Thoracoscopic view of an endometrial implant (arrows).

Similar to pelvic endometriosis, thoracic endometriosis may show different signal intensities on T1 and T2 images, depending on the stage of the lesion [23]. However, a pleural-based lesion exhibiting homogeneous high signal intensity on T1-and T2-weighted images is distinctive of pleural endometriosis. MRI can be used to identify

endometriomas, which appear as hyperintense nodules. In some cases, the diffusion restriction in diffusion-weighted imaging can be useful in detecting small endometriomas. Pleural effusion can also show signal hyperintensity on T1 sequences, probably due to the blood component of fluid [17,21]. MRI after drainage of pleural effusion and coinciding with menses could support this diagnosis in women with catamenial hemothorax or hemopneumothorax [22,24].

Pleural (visceral or parietal) and diaphragmatic endometriosis is characterized by the presence of both endometrial stroma and glands in the form of blue-brown implants or "chocolate cysts," almost invariably associated with hemorrhage, fibrosis, and inflammatory infiltrates to various extents. Most cases of pleural involvement exhibit a nodular or nodulocystic pattern associated with pleural thickening, adhesions, and hemorrhage. Endometriotic foci rarely appear as dark-red dimples, less than 5 mm in diameter. In some cases, endometriotic foci can be identified only in deeper sections [6].

The most effective treatment strategy for thoracic endometriosis remains controversial due to lack of therapeutic trial data available for this uncommon entity [25]. Treatment includes video-assisted thoracoscopy for resection of endometrial implants along with talc pleurodesis to help prevent recurrence. In cases of diaphragmatic involvement, diaphragmatic resection should also be considered. Surgical treatment in combination with at least 6 months of clinical treatment, including hormone-modulating agents to suppress proliferation of endometrial implants, has been shown to improve prognosis [26]. Clinical treatment includes the administration of gonadotropin-releasing hormone analogs with the aim of suppressing endometrial tissue by blocking the action of estrogen. High recurrence rates of up to 50% have been reported with this therapy. Because this treatment precludes pregnancy and has side effects such as virilization and weight gain, it is unacceptable to some women [7].

3. Thoracic splenosis

Thoracic splenosis is a rare condition that involves the autotransplantation of splenic tissue into the chest, usually after combined splenic and diaphragmatic injury [27]. This condition is commonly accompanied by abdominal splenosis. It has been found in approximately 18% of patients after combined diaphragmatic injury and splenic rupture [28].

The mechanism underlying autotransplantation begins with splenic rupture, due to trauma or surgical removal. The spillage of damaged splenic pulp into adjacent cavities is presumed to begin the seeding process. A second mechanism is the hematogenous spread of splenic pulp, as suggested by case reports of intrahepatic and intracranial splenosis [29].

Thoracic splenosis has a male predominance of more than 3:1, likely attributable to the higher rate of trauma in young men than in women [30]. The average interval between the causal event and detection of thoracic splenosis is 21 years, with a range of 3–45 years [30]. It is usually asymptomatic and thus is most commonly an incidental finding when imaging is performed for other reasons [30]. Rarely, thoracic splenosis causes chest pain or hemoptysis [31–34]. Thoracic splenosis should be considered in the setting of solitary or multiple left pleural nodules and evidence of remote splenic trauma (i.e., splenectomy or splenules in the left upper quadrant) [28]. Splenic implants typically appear as multiple small pleural or subpleural nodules up to 3 cm in diameter, although some may be larger and form masses [35].

The diagnosis of thoracic splenosis is difficult and requires the presence of a detailed history as well as a high index of suspicion. Despite occasional reports of splenosis diagnosed only by nuclear medicine studies, some authors agree that definitive diagnosis requires cytologic or histologic examination [36,37]. Most authors have reported that fine-needle aspiration is of little utility, due to its low sensitivity [38]. Transthoracic fine-needle-aspiration cytology of thoracic splenosis may create pitfalls in diagnostic interpretation when populations of small and medium lymphocytes erroneously suggest a lymphoproliferative disorder [36]. When less-aggressive techniques fail, surgery must be undertaken to rule out malignancy. Video-assisted thoracic surgery is a relatively recent adaptation of minimal-access surgery for the examination of pleural lesions [37].

Chest radiography and CT show splenic implants as multiple, small, pleural or subpleural nodules up to 3 cm in diameter (Fig. 2), although some may be larger and form masses [39,40]. Uncomplicated cases are not associated with pleural effusion. On CT, the lesions in splenosis show contrast enhancement that is identical to that of the spleen [2]. The density of the splenic implants (in Hounsfield units) is similar to that of normal spleen [28]. Radiological follow-up may show slow growth or regression of the nodules [39].

On MRI, the lesions have signal intensity and enhancement characteristics identical to those of normal spleen. They are isointense to muscle on T1-weighted images and slightly hyperintense on T2-weighted images [41], and show significant contrast enhancement immediately after the application of gadodiamide [42]. Standard MRI is not useful in narrowing the differential diagnosis. Ferumoxide-enhanced MRI may be an alternative imaging procedure to prove the presence of splenic tissue. Ferumoxides are superparamagnetic iron oxides (SPIOs) that are cleared by the reticuloendothelial system. In magnetic fields, large SPIOs cause strong local field inhomogeneities with shortening of T2 and T2* relaxation. Ten minutes after intravenous application of ferumoxide particles, all splenotic lesions show pronounced signal loss on T2* sequences. The signal loss is even more pronounced 1 h after the application of ferumoxides [42,43].

The diagnosis of thoracic splenosis can be confirmed by using scintigraphy with technetium 99 m (99mTc)-sulfur colloid, indium 111–labeled platelets, or 99mTc-tagged heat-damaged red blood cells, with the latter being more sensitive and specific [30]. Single-photon emission CT studies have shown significant superiority over planar scintigraphy in diagnostic performance. The better resolution of tomographic techniques allows the demonstration of smaller nodules of residual tissue [44].

Splenic implants are reddish-blue nodules that may be sessile or pedunculated. Their number ranges from only a few to hundreds, and their size ranges from a few millimeters to several centimeters [31]. In splenosis, tissue usually shows distorted architecture with no hilum and a poorly formed capsule; tissue may be of any shape and size. Furthermore, the histology of splenosis can be quite varied. Most reports have described the tissue as lacking trabecular structure, with less elasticity than normal spleen, and poorly formed or deficient white pulp with normal-appearing red pulp [31]. Splenic implants derive their blood supplies from new arteries that penetrate the capsule. The capsules of splenotic nodules are derived from surrounding reactive granulation and fibrous tissues, and are usually devoid of smooth muscle and elastic tissue components. These components are seen in accessory spleens [45].

Removal of splenosis, although necessary for diagnosis, may be detrimental to the patient. Whether splenosis can restore normal immunologic function of the spleen remains unknown. Some authors have argued that a small amount of splenic tissue is insufficient to protect patients from overwhelming postsplenectomy sepsis [46]. However, other studies identified normal circulating antibody levels and response to *S. pneumonia* antigens within normal limits [47]. In view of this controversy and the potential

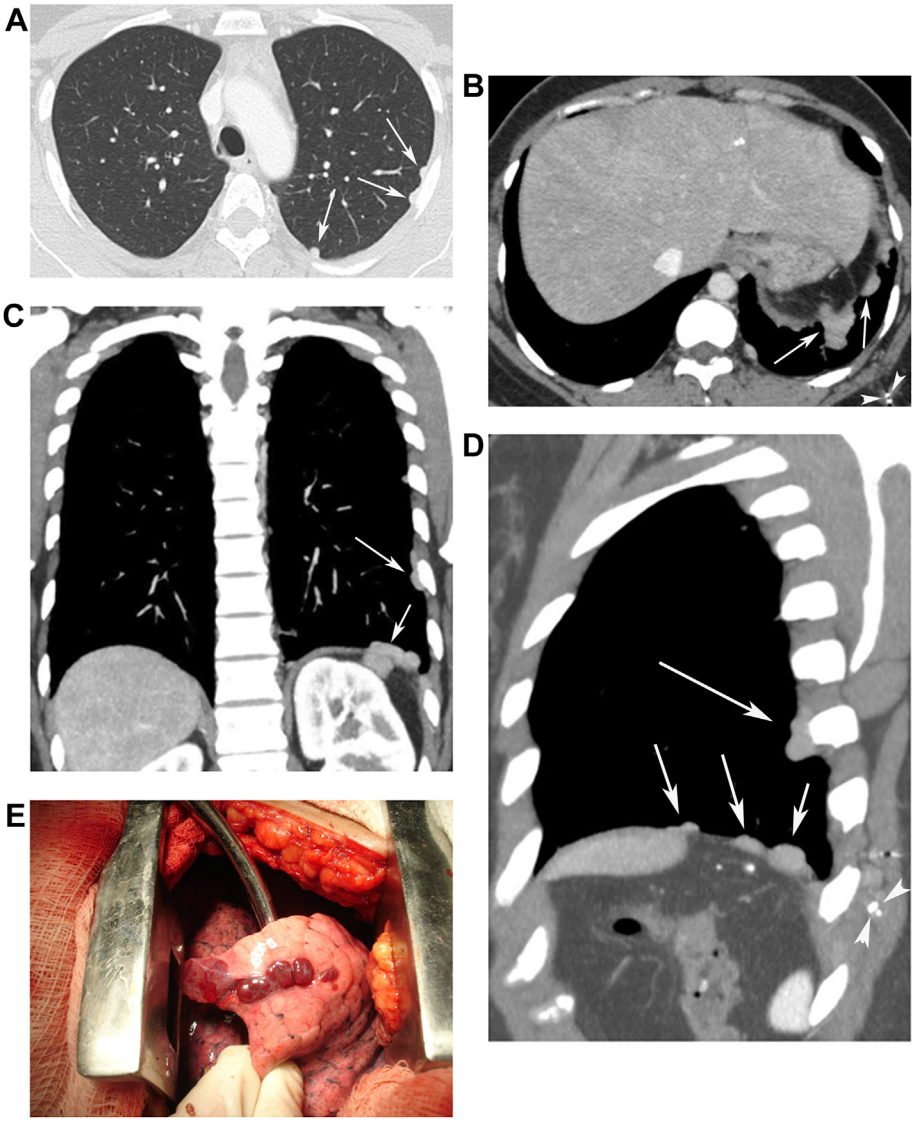

Fig. 2. An asymptomatic 58-year-old woman with thoracic splenosis. She reported a history of a gunshot wound that transfixed the thoracoabdominal region 40 years previously. Computed tomography (A–D) shows a lobulated pleural mass and well-circumscribed pleural-based nodules in the left hemithorax (arrows). Note also the absence of the spleen in the left upper quadrant, a nodular opacity that corresponds to a residual spleen parenchyma, and metallic bullet fragments in the chest wall (arrowheads). Thoracotomy (E) disclosed multiple reddish-purple nodules on the pleural surface (Fig. 1E reprinted with permission from Marchiori E, Rodrigues RS, Reis MC, Zanetti G, Menna Barreto M. Pleural nodules in a patient with a colonic tumor. Thorax 2014; 69 (4):395–398).

benefit of splenic nodules, some authors advocate removal of only a minimum of autotransplanted tissue for diagnosis, rather than excision of all nodules [37].

4. Thoracolithiasis

Thoracolithiasis is a condition in which one or more free bodies with or without calcification are freely mobile in a pleural cavity, without a history of previous trauma, pleurisy, or iatrogenic intervention [48]. Some authors have described thoracolithiasis as a mobile calcified nodular opacity in the pleural space [49].

The exact etiology of thoracolithiasis is unknown, but based on pathologic findings, some explanations for its formation have been proposed: 1) movement of pleural or pericardial fat into the intrathoracic space, 2) tearing off of a pleural or peripheral pulmonary lipoma, 3) focus of old pulmonary tuberculosis, and 4) aggregation of macrophages phagocytosing dust [50,51]. Given the left-sided predominance (70%) of this entity, fat necrosis in the epipericardial space has also been proposed as a likely cause [48,51]. Thoracolithiasis is rarely symptomatic, and most cases are discovered incidentally on radiographs, CT images, or at the time of surgery [52]. The diagnosis of thoracolithiasis can be suspected by imaging findings, especially the demonstration of mobility of a calcified pleural nodule (Fig. 3), but it can be confirmed only by surgical excision and histopathologic analysis.

Larger pleural stones can be seen on plain radiographs, but CT plays the most central role in diagnosis. In particular, CT helps to confirm calcified density when the density of the nodule is indeterminate on conventional radiography. Stone size ranges from 5 to 15 mm, and stones occur more frequently in the left than in the right pleural cavity. The stones are usually ovoid and smoothly marginated, with different locations on serial scans due to mobility. They are most often found in the dependent part of the pleural cavity, presumably secondary to the effect of gravity, especially on the surface of the diaphragm, on the chest wall adjacent to the lower lung, abutting the left cardiac margin, or near the paraspinal

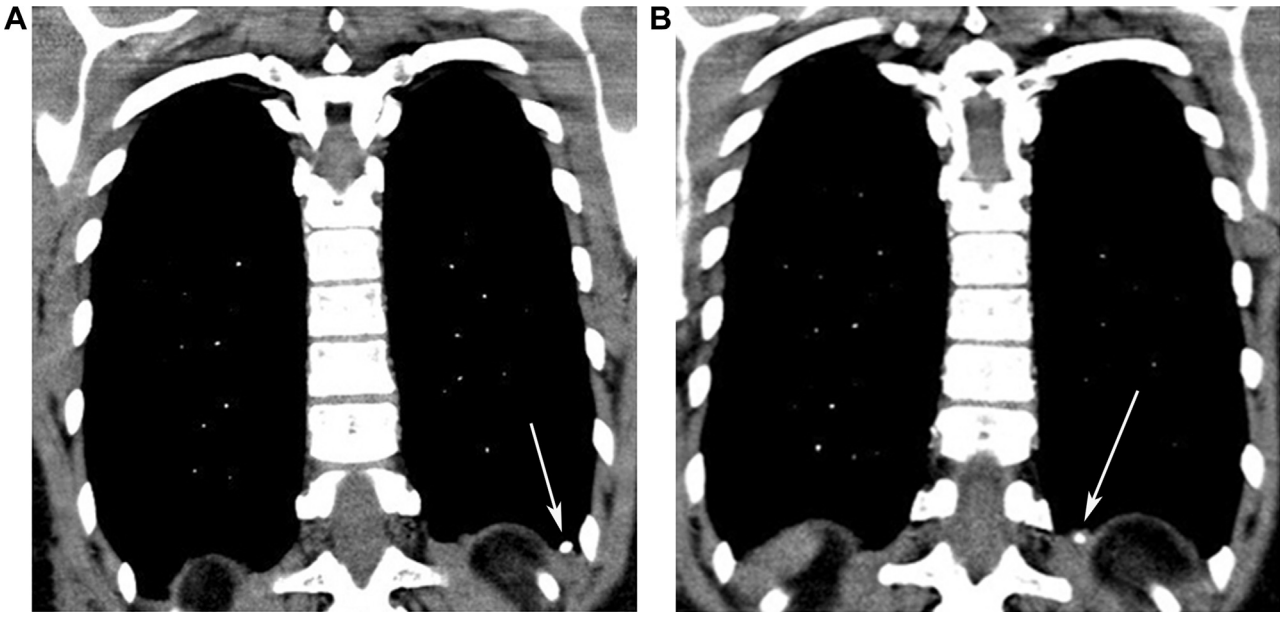

Fig. 3. An asymptomatic 50-year-old man with thoracolithiasis. A. Initial coronal chest computed tomography shows a calcified nodule at the left costophrenic angle (arrow). B. A second chest computed tomography examination shows medial movement of the nodule (arrow).

space. The demonstration of mobility on serial imaging confirms thoracolithiasis [53].

Most stones are calcified, with or without low central density due to the presence of fat [52]. Calcification can be diffuse and homogeneous, peripheral with an eggshell-like appearance, or spotty and central [49]. Although calcification is a common finding, thoracolithiasis has been described without this feature [49,54]. Less-calcified or immobile thoracolithiasis is clinically important because it is often misdiagnosed and unnecessarily surgically resected. Moreover, some thoracoliths have been reported to enlarge on follow-up and may be difficult to distinguish from neoplastic disease [49]. On T1-and T2-weighted MR images of the chest, these diffuse calcified nodules present with central areas of high intensity, with an appearance like soft cloth, probably due to the presence of fat [49,54]. The differential diagnosis includes fibrin bodies, foreign body granulomas, and gallstone spillage into the pleural space following cholecystectomy [51].

Histopathologically, fibrous tissue, with or without hyalinization, surrounding a central core is found in most cases. The composition of the central core is variable, but most cases exhibit fat with or without calcification or necrosis; less-common findings are dust, stones, and denatured blood and fibrin [49,52]. Thoracolithiasis does not require treatment or intervention, except in the presence of clearly associated symptoms [51].

5. Retained foreign objects (Textiloma)

The term “textiloma”, also called “gossypiboma”, describes a mass in the body that is composed of a cotton matrix surrounded by a foreign body reaction [55,56]. Although this condition is generally reported after abdominal laparotomy, a gossypiboma can occur following any surgical procedure [56]. This condition is underreported in the literature due to medicolegal consequences. Textiloma may be asymptomatic or present as chronic pain, infection, and abscess [56,57].

Textiloma may be asymptomatic or present with fever, cough, hemoptysis, and weight loss [55,56]. It is associated with numerous complications (abscesses, fistulas, perforations, adhesions, migrations within contiguous organs, or remobilization through vessels) [58,59]. Textilomas can be diagnosed based on previous operative history and imaging findings, and confirmed by surgical excision [58]. The demonstration of cotton fibers in gossypiboma samples obtained by transthoracic needle biopsy has been reported [56].

Radiography is used initially for the detection of retained sponges. Although many surgical swabs have been labeled with radiopaque markers to facilitate their detection by imaging techniques since the 1980s, the diagnosis of gossypiboma is not always easy. The markers may be distorted by folding, twisting, or disintegration over time [55]. A plain chest radiograph usually shows a peripheral or paramediastinal mass with an incomplete border sign, suggesting an extraparenchymal location [56,60]. Thoracic textilomas may present on radiographs as heterogeneous or homogeneous pleural opacities with or without trapped air bubbles, or as mediastinal opacities [58,61]. Radiographs can also suggest the diagnosis when a characteristic whirl-like pattern is present [59]. Chest radiographs may also be normal [61]. On ultrasound, a textiloma may also present in various ways: as an echogenic area with a sharply delineated acoustic shadow, a hypoechoic mass with or without a complex cystic pattern, a cystic mass with irregular internal components, or a complex mass with hyper- and hypoechoic regions [61,62]. The acoustic shadows are too strong and extensive to be explained by gas or calcification revealed by CT [62].

CT is the most effective method for the detection of a retained surgical sponge in the chest [56,63]. The manifestations of textilomas on CT vary according to the location and chronicity of the gauze sponges, and the types of reaction that they cause in the body [56]. In the early postoperative period, CT characteristically shows a well-defined mediastinal or pleural-based soft-tissue mass with a hyperdense rim (Fig. 4), central air bubbles, and a whirl-like pattern consisting of curvilinear, high-density stripes [56,64]. Peripheral enhancement is observed following the administration of contrast. The spongiform appearance of a textiloma represents air bubbles trapped within the fibers of the gauze sponge in liquid media. Lamellar, high-density areas represent the sponge itself [56]. The absence of central enhancement is probably due to the presence of a clot trapped within the sponge, and peripheral enhancement is caused by an inflammatory reaction [63]. The air trapped by the foreign material is resorbed overtime, and in the absence of a

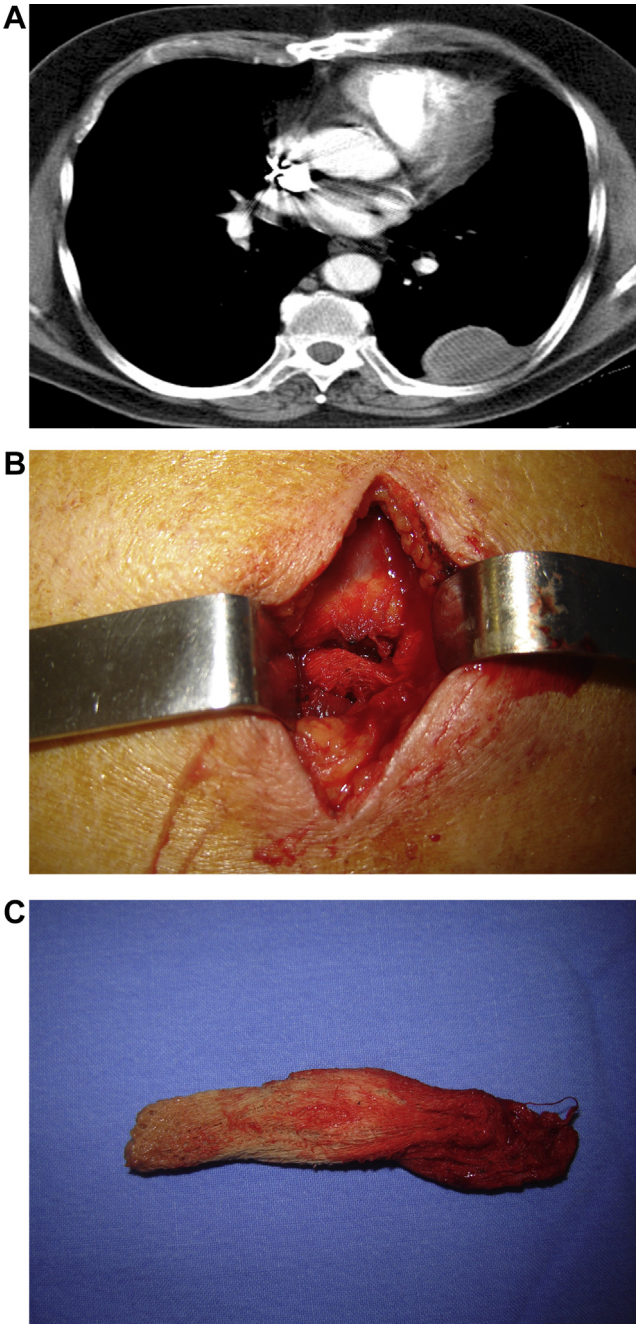

Fig. 4. A 54-year-old woman with a thoracic textiloma. A chest computed tomographyimage obtained with the mediastinal window setting (A) reveals a well-defined, hypodense pleural mass in the left hemithorax with a hyperdense peripheral rim. (B,C) A foreign textile body (gauze) was surgically excised from the pleural cavity (Reprinted with permission from Nobre LF, Marchiori E, May F, Carrão AD Jr., Zanetti G, Machado DM. Thoracic textilomas after myocardial revascularisation: typical CT findings. Br J Radiol. 2010; 83 (985):4–7).

radiopaque marker, lesions appear as solid masses with or without whirl-like, high-density stripes in the late postoperative period [65]. Differentiation from other masses is difficult at this stage, even with knowledge of a prior surgery [56]. Air bubbles may not be as prominent for intrathoracically as for intra-abdominally retained sponges. Resorption of air by the pleura is a likely explanation for this difference [63,65]. Cystic masses with an unfolded pattern, strongly suggesting the appearance of a towel, have also been described [66]. Other CT features of pleural textilomas are less specific. This body may appear as a complex pleural-based mass with concentric layers of different densities, a mass with a high-density component, or a calcified pleural mass [63]. Some authors have argued that MRI is more effective than CT for the examination of textilomas. On MRI, the mass is hypointense in T1 sequences and hyperintense in T2 sequences, with a surrounding capsule corresponding to thick fibrous tissue [61]. On T2-weighted images, low-signal-intensity structures with wavy, striped, and/or spotted appearances within the mass have also been described [59]. The presence of a T2-hypointense spotted serpiginous structure in the center of the mass is related to the foreign body.

In the presence of a textiloma, cells involved in a foreign body reaction, especially macrophages, begin the formation of granulation tissue consisting of fibroblasts and angioblasts in a matrix of collagen. The mass of phagocytes encapsulates the foreign body with a dense membrane of connective tissue. Over time, this localized lesion can undergo caseation necrosis, calcification, and/or liquefaction. After fibrous encapsulation has occurred, the lesion is generally referred to as a granuloma. In addition, a zone of macrophages, lymphocytes, and granulocytes is present around the giant cells and outermost encapsulating membrane of fibrous tissue [58].

For a gossypiboma that remains asymptomatic, the therapeutic approach must balance the potential risk of evolution of the foreign body with that of the surgical procedure [67]. Although surgery is the recommended mode of treatment, prevention is the best course and should be emphasized. Prevention can be facilitated by implementation of measures such as meticulous counting of all surgical materials, thorough exploration of the surgical site at the conclusion of a procedure, and routine use of surgical textile materials impregnated with a radiopaque marker [67,68].

6. Pleural plaques

Exposure to asbestos is an important public health hazard in all industrial societies [69]. Pleural plaques are the most common manifestation of asbestos-related disease, which has an extremely long latency (typically 20–30 years after the onset of exposure) [3,70,71]. They appear as discrete, circumscribed areas of hyaline or calcified fibrosis. Pleural plaques are useful as a marker of exposure and are not usually associated with symptoms or functional impairment [3,69]. They are benign, with no risk of malignant degeneration and no follow-up treatment requirement [3,70].

The pathogenesis of plaques is uncertain, but it is thought to involve the transportation of fibers to the pleural space via the lymphatic system, which prompts an inflammatory reaction that leads to hyaline fibrosis along the parietal pleural surface. Another proposed mechanism involves the hematogenous route [3,70].

The classic distribution of the plaques includes the parietal pleura, with a predilection for the diaphragmatic dome and the undersurfaces of the lower posterolateral ribs. The apices and costophrenic angles are typically spared [3,69,71].

CT is the modality of choice for the assessment of pleural plaques, as it is more sensitive and specific than plain radiography. CT may show anterior and paravertebral plaques that are not well visualized by chest radiography. Calcification is depicted in 10–15% of cases by radiography and in 15–20% of cases by CT [3]. On high-resolution CT, pleural plaques appear as well-circumscribed areas of pleural thickening separated from the underlying ribs and extrapleural fat by a thin layer of fat (Fig. 5) [71].

Although plaques almost always involve the parietal pleura, they occasionally arise from the visceral pleura. When visceral plaques are present, they are typically associated with underlying parenchymal abnormalities, including short interstitial lines that radiate from the plaques (so-called “hairy” plaques) or more extensive parenchymal opacities [3,70].

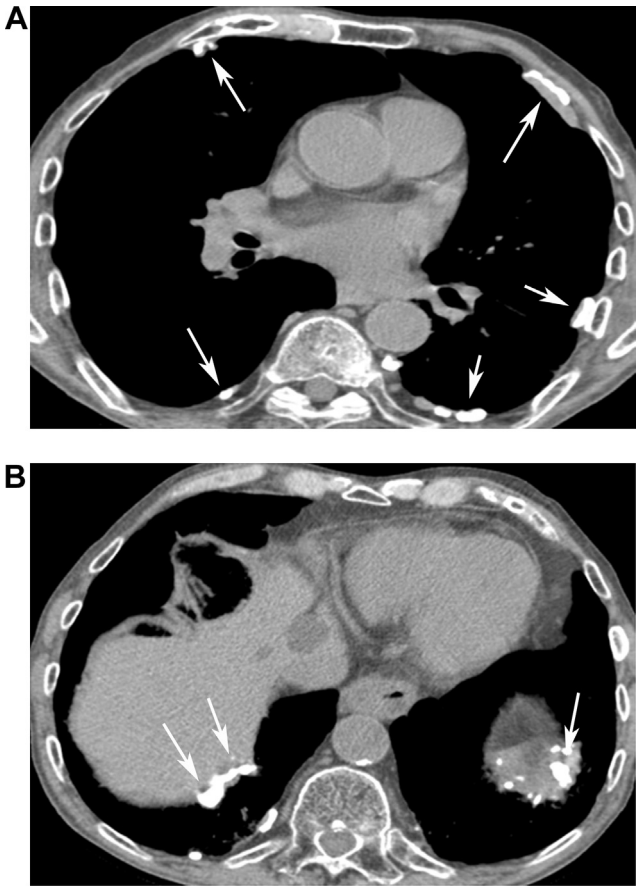

Fig. 5. Asbestos-related pleural plaques in a 69-year-old man. Axial computed tomography images (mediastinal window settings) obtained at the levels of the lower lobes (A) and diaphragmatic region (B) show multiple nodular and elongated calcified plaques located along the lateral pleural surface (arrows in A), and the dome of the diaphragm (arrows in B).

On gross examination, plaques are tan-white with smooth or nodular surfaces. Microscopically, the plaques are composed of dense hyalinized collagen with a "basket-weave" appearance and are relatively acellular. Asbestos fibers (usually chrysotile) are often seen, but asbestos bodies are usually absent [69,70].

Diffuse pleural thickening is seen less frequently than pleural plaques following exposure to asbestos. It is defined as a smooth, uninterrupted pleural density extending over at least one-fourth of the chest wall, with or without costophrenic angle obliteration [69].

7. Pleural pseudotumor

The term "pleural pseudotumor," or "vanish tumor" may be used to describe a well-demarcated collection of pleural fluid contained within an interlobar pulmonary fissure or in a subpleural location adjacent to a fissure, which may be diagnosed erroneously as pleural or parenchymal lung nodules or masses [3,72].

Pseudotumors usually manifest as incidental radiographic findings in patients with disorders associated with transudative effusions, especially congestive heart failure. Others causes of transudates include hypoalbuminemia, cirrhosis, and renal insufficiency [3,72].

Under normal conditions, the adjacent lung applies a similar retractile force to the entire pleural space. In the presence of pleural effusion, the elastic recoil of the lung causes each lobe to retract toward the hilum. This tension determines fissure widening and can draw fluid into the fissure, even in nondependent locations. The minor fissure is most affected, as the middle lobe is the minor lobe and has the greatest tendency to retract [3,72].

Misdiagnosis of a pseudotumor as a parenchymal lung or pleural lesion may lead to unnecessary patient anxiety; costly imaging studies; invasive procedures, including attempted tissue biopsies; and inappropriate empiric trials of antibiotics [72].

Pseudotumors may be diagnosed, presumptively, on chest radiographs based on their typical lenticular or biconvex contours, tapering ends, sharp margins, and location along the courses of interlobar fissures. The concurrent presence of a dependent pleural effusion aids recognition of a pleural pseudotumor [3]. CT may better demonstrate the pseudotumor's liquid content and its relationship to fissures (Fig. 6) ([3,72,73]). The Hounsfield unit characteristic of the effusion was similar to that of freely layering liquid in the contralateral hemithorax, and the effusion was shown to be transudate [72].

More than three-fourths of reported cases were in the right horizontal fissure. Infrequently, it occurs in the horizontal and oblique fissures simultaneously [72].

Incorrect diagnosis of a pulmonary pseudotumor is commonly due to the analysis of a chest radiograph obtained from the anteroposterior, rather than lateral, view. The appearance of an encapsulated effusion in the major fissure on a frontal-view radiograph is often nonspecific and less characteristic, as it produces a veil of opacity with indistinct borders. A lateral-view radiograph is more likely to yield a correct diagnosis [72].

The management of interlobar effusions consists of treatment of the underlying disorder, including standard management for pleural effusions ([72,73]). The interlobar pleural fluid and the tumorlike appearance it produces disappear with therapy for heart failure ([73]).

8. Conclusion

The diagnosis of focal tumorlike conditions is facilitated by the recognition of certain imaging patterns and interpretation of these patterns in the clinical context. Thoracic endometriosis with CP should be considered in a woman of childbearing age who presents

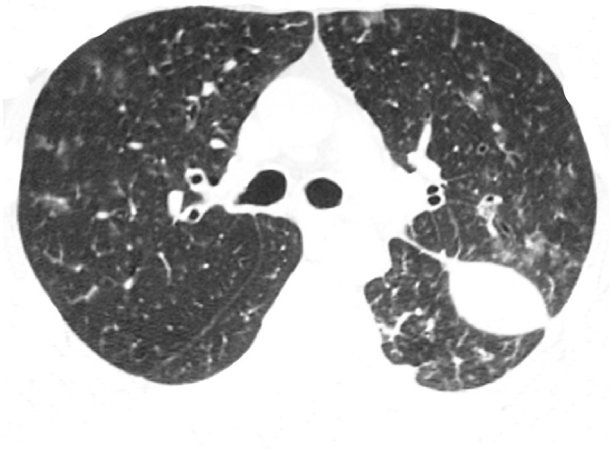

Fig. 6. A 52-year-old woman with heart failure and a pleural pseudotumor. Axial computed tomography image (lung window settings) obtained at the level of bronchial bifurcation shows a sharply circumscribed, homogeneous opacity in the left hemithorax. The opacity is elliptical; with tapering ends situated in keeping with the position of the major fissure. The pseudotumor disappeared completely after 2 weeks of appropriate therapy.

with recurrent pneumothorax or hydropneumothorax occurring at or around the onset of menses. Pleural nodules corresponding to endometriotic implants can be found on imaging studies. Thoracic splenosis should be considered in a patient who has a history of thoracoabdominal trauma, an absent spleen, and left pleural nodules. Thoracolithiasis should be considered especially in the presence of mobile calcified pleural nodules. Textiloma should be considered in a patient with a history of previous surgery upon the detection of a pleural opacity with or without trapped air bubbles or whirl-like pattern. Pleural plaques typically appear on the diaphragmatic dome and lower posterolateral ribs in a patient with an epidemiological history of asbestos exposure. Pleural pseudotumor may be diagnosed based on typical morphology and location along interlobar fissures; this diagnosis is aided by the concurrent presence of a pleural effusion.

Conflict of interest statement

All authors declare that they have no conflict of interest.

References

[1] H.M. Salahudeen, E.T. Hoey, R.J. Robertson, M.J. Darby, CT appearances of pleural tumours, Clin. Radiol. 64 (9) (2009) 918–930.
[2] T. Hussein-Jelen, A.A. Bankier, R.L. Eisenberg, Solid pleural lesions, AJR Am. J. Roentgenol. 198 (6) (2012) W512–W520.
[3] C.M. Walker, J.E. Takasugi, J.H. Chung, G.P. Reddy, S.L. Done, S.N. Pipavath, R.A. Schmidt, J.D. Godwin 2nd, Tumor like conditions of the pleura, Radiographics 32 (4) (2012) 971–985.
[4] D.L. Olive, L.B. Schwartz, Endometriosis, N. Engl. J. Med. 328 (24) (1993) 1759–1769.
[5] J. Joseph, S.A. Sahn, Thoracic endometriosis syndrome: new observations from an analysis of 110 cases, Am. J. Med. 100 (2) (1996) 164–170.
[6] A. Augoulea, I. Lambrinoudaki, G. Christodoulakos, Thoracic endometriosis syndrome, Respiration 75 (1) (2008) 113–119.
[7] N.P. Ghonge, S. Saxena, P. Bhargava, Imaging findings and management strategies in pleural endometriosis, Clin. Pulm. Med. 20 (1) (2013) 48–50, http://dx.doi.org/10.1097/CPM.0b013e31827a2fc2.
[8] D.B. Flieder, C.A. Moran, W.D. Travis, M.N. Koss, E.J. Mark, Pleuro-pulmonary endometriosis and pulmonary ectopic deciduosis: a clinicopathologic and immunohistochemical study of 10 cases with emphasis on diagnostic pitfalls, Hum. Pathol. 29 (12) (1998) 1495–1503.
[9] P. Rousset, C. Rousset-Jablonski, M. Alifano, A. Mansuet-Lupo, J.N. Buy, M.P. Revel, Thoracic endometriosis syndrome: CT and MRI features, Clin. Radiol. 69 (3) (2014) 323–330.
[10] M. Alifano, R. Trisolini, A. Cancellieri, J.F. Regnard, Thoracic endometriosis: current knowledge, Ann. Thorac. Surg. 81 (2) (2006) 761–769.
[11] E. van der Merwe, M.M. Schuurmans, F. de Kock, I. Siebert, C. Wright, C.T. Bolliger, Bloodstained pleural effusion in a 38-year-old non-smoking female, Respiration 72 (1) (2005) 101–104.
[12] S. Korom, H. Canyurt, A. Missbach, D. Schneiter, M.O. Kurrer, U. Haller, P.J. Keller, M. Furrer, W. Weder, Catamenial pneumothorax revisited: clinical approach and systematic review of the literature, J. Thorac. Cardiovasc Surg. 128 (4) (2004) 502–508.
[13] J.G. Im, H.S. Kang, B.I. Choi, J.H. Park, M.C. Han, C.W. Kim, Pleural endometriosis: CT and sonographic findings, AJR Am. J. Roentgenol. 148 (3) (1987) 523–524.
[14] Y.R. Lee, Y.W. Choi, S.C. Jeon, S.S. Paik, J.H. Kang, Pleuropulmonary endometriosis: CT-pathologic correlation, AJR Am. J. Roentgenol. 186 (6) (2006) 1800–1801.
[15] S.Y. Chung, S.J. Kim, T.H. Kim, W.G. Ryu, S.J. Park, D.Y. Lee, H.C. Paik, H.J. Kim, S.H. Cho, J.K. Kim, K.J. Park, Y.H. Ryu, Computed tomography findings of pathologically confirmed pulmonary parenchymal endometriosis, J. Comput Assist. Tomogr. 29 (6) (2005) 815–818.
[16] Y.J. Hong, H.C. Paik, H.J. Kim, D.Y. Lee, S.J. Kim, S.H. Cho, Y.M. Oh, A case of parenchymal pulmonary endometriosis, Yonsei Med. J. 40 (5) (1999) 514–517.
[17] E. Marchiori, G. Zanetti, P.P. Rafful, B. Hochhegger, Pleural endometriosis and recurrent pneumothorax: The role of magnetic resonance imaging, Ann. Thorac. Surg. 93 (2012) 696–697.
[18] J.R. Volkart, CT findings in pulmonary endometriosis, J. Comput Assist. Tomogr. 19 (1) (1995) 156–157.
[19] M.J. Ciudad, N. Santamaría, A. Bustos, J. Ferreirós, B. Cabeza, A. Gómez, Imaging findings in catamenial pneumothorax, Radiologia 49 (2007) 263–267.
[20] E. Marchiori, B. Hochhegger, G. Zanetti, Thoracic endometriosis: the role of imaging, Arch. Bronconeumol (2014 Nov 3), http://dx.doi.org/10.1016/j.arbres.2014.04.013.
[21] E. Marchiori, G. Zanetti, R.S. Rodrigues, L.S. Souza, A.S. Souza Junior, F.A. Francisco, B. Hochhegger, Pleural endometriosis: findings on magnetic resonance imaging, J. Bras. Pneumol. 38 (6) (2012) 797–802.
[22] G. Picozzi, D. Beccani, F. Innocenti, M. Grazzini, M. Mascalchi, MRI features of pleural endometriosis after catamenial haemothorax, Thorax 62 (8) (2007) 744.
[23] A. Coutinho Jr., L.K. Bittencourt, C.E. Pires, F. Junqueira, C.M. Lima, E. Coutinho, M.A. Domingues, R.C. Domingues, E. Marchiori, MR imaging in deep pelvic endometriosis: a pictorial essay, Radiographics 31 (2) (2011) 549–567.
[24] P.C. Cassina, M. Hauser, G. Kacl, B. Imthurn, S. Schröder, W. Weder, Catamenial hemoptysis. Diagnosis with MRI, Chest 111 (5) (1997 May) 1447–1450.
[25] Z. Yu, J.K. Fleischman, H.M. Rahman, A.F. Mesia, F. Rosner, Catamenial hemoptysis and pulmonary endometriosis: a case report, Mt. Sinai J. Med. 69 (4) (2002) 261–263.
[26] P. Athwal, K. Patel, C. Hassani, S. Bahadori, P. Nardi, A case of multisystem endometriosis, J. Radiol. Case Rep. 7 (10) (2013) 1–6.
[27] E. Sahin, S. Karadayi, A. Nadir, M. Kaptanoglu, Thoracic splenosis accompanied by diaphragmatic hernia, Can. J. Surg. 52 (6) (2009) E293–E294.
[28] J.P. Normand, M. Rioux, M. Dumont, G. Bouchard, L. Letourneau, Thoracic splenosis after blunt trauma: frequency and imaging findings, AJR Am. J. Roentgenol. 161 (4) (1993) 739–741.
[29] J.F. Cordier, J.P. Gamondes, P. Marx, I. Heinen, R. Loire, Thoracic splenosis presenting with hemoptysis, Chest 102 (2) (1992) 626–627.
[30] J.N. Yammine, A. Yatim, A. Barbari, Radionuclide imaging in thoracic splenosis and a review of the literature, Clin. Nucl. Med. 28 (2) (2003) 121–123.
[31] R.D. Fremont, Rice TW Splenosis: a review, South Med. J. 100 (6) (2007) 589–593.
[32] G. Gaedcke, K. Storz, S. Braun, H.P. Horny, Thoracic splenosis with symptoms of coronary heart disease, Dtsch. Med. Wochenschr 124 (33) (1999) 958–961.
[33] S. Fukuhara, S. Tyagi, J. Yun, M. Karpeh, A. Reyes, Intrathoracic splenosis presenting as persistent chest pain, J. Cardiothorac. Surg. 7 (2012) 84.
[34] K. Gopal, M.T. Jones, S.M. Greaves, An unusual cause of chest pain, Chest 125 (4) (2004) 1536–1538.
[35] J.V. O'Connor, C.C. Brown, J.K. Thomas, J. Williams, E. Wallsh, Thoracic splenosis, Ann. Thorac. Surg. 66 (2) (1998) 552–553.
[36] M.F. Naylor, N. Karstaedt, S.J. Finck, O.L. Burnett, Noninvasive methods of diagnosing thoracic splenosis, Ann. Thorac. Surg. 68 (1) (1999) 243–244.
[37] R.A. Beekman, B. Louie, R. Singh, S. Salama, J.D. Miller, Asymptomatic thoracic splenosis after thoracoabdominal trauma: establishing a diagnosis, Inj. Extra 36 (7) (2005) 283–286, http://dx.doi.org/10.1016/j.injury.2004.12.050.
[38] E. Ruffini, S. Asioli, P.L. Filosso, R. Senetta, L. Macrì, A. Cavallo, A. Oliaro, Intrathoracic splenosis: a case report and an update of invasive and noninvasive diagnostic techniques, J. Thorac. Cardiovasc Surg. 134 (6) (2007) 1594–1595.
[39] A.D. Mançano, G. Zanetti, B.C. Duarte, L.F. Prado, E. Marchiori, Thoracic splenosis after thoracoabdominal trauma presenting as pleural nodules, Lung 190 (2012) 699–701.
[40] E. Marchiori, R.S. Rodrigues, M.C. Reis, G. Zanetti, M. Menna Barreto, Pleural nodules in a patient with a colonic tumor, Thorax 69 (4) (2014) 395–398.
[41] R.P. Bordlee, N. Eshaghi, O. Oz, Thoracic splenosis: MR demonstration, J. Thorac. Imaging 10 (2) (1995) 146–149.
[42] H. Prosch, E. Oschatz, E. Pertusini, G. Mostbeck, Diagnosis of thoracic splenosis by ferumoxides-enhanced magnetic resonance imaging, J. Thorac. Imaging 21 (3) (2006) 235–237.
[43] M. Ishibashi, Y. Tanabe, H. Miyoshi, E. Matusue, T. Kaminou, T. Ogawa, Intrathoracic splenosis: evaluation by superparamagnetic ironoxide-enhanced magnetic resonance imaging and radionuclide scintigraphy, Jpn. J. Radiol. 27 (9) (2009) 371–374.
[44] I. Gunes, T. Yilmazlar, I. Sarikaya, T. Akbunar, C. Irgil, Scintigraphic detection of splenosis: superiority of tomographic selective spleen scintigraphy, Clin. Radiol. 49 (2) (1994) 115–117.
[45] C.R. Fleming, E.R. Dickson, E.G. Harrison Jr., Splenosis: autotransplantation of splenic tissue, Am. J. Med. 61 (3) (1976) 414–419.
[46] K. Hansen, D.B. Singer, Asplenic-hyposplenic overwhelming sepsis: post-splenectomy sepsis revisted, Pediatr. Dev. Pathol. 4 (2001) 105–121.
[47] J.M. Hathaway, R.A. Harley, S. Self, G. Schiffman, G. Virella, Immunolgical function in post-traumatic splenosis, Clin. Immun. Immunopathol. 74 (1995) 143–150.
[48] S. Kosaka, N. Kondo, H. Sakaguchi, T. Kitano, T. Harada, K. Nakayama, Thoracolithiasis, Jpn. J. Thorac. Cardiovasc Surg. 48 (5) (2000) 318–321.
[49] F. Kinoshita, Y. Saida, Y. Okajima, S. Honda, T. Sato, A. Hayashibe, S. Hiramatsu, Thoracolithiasis: 11 cases with a calcified intrapleural loose body, J. Thorac. Imaging 25 (1) (2010) 64–67.
[50] T. Tsuchiya, K. Ashizawa, T. Tagawa, S. Tsutsui, N. Yamasaki, T. Miyazaki, T. Hayashi, T. Nagayasu, A case of migrated thoracolithiasis, J. Thorac. Imaging 24 (4) (2009) 325–327.
[51] J. Strzelczyk, B.J. Holloway, P.G. Pernicano, A.M. Kelly, Rollingstones in the pleural space: thoracoliths on CT, and a review of the literature, Clin. Radiol. 64 (1) (2009) 100–104.
[52] S. Peungjesada, P. Gupta, A.M. Mottershaw, Thoracolithiasis: a case report, Clin. Imaging 36 (3) (2012) 228–230.
[53] R. Bhayana, Y.A. Chen, D.P. Deva, Bilateral mobile thoracolithiasis, J. Radiol. Case Rep. 8 (9) (2014) 16–20.

[54] D. Tanaka, H. Niwatsukino, F. Fujiyoshi, M. Nakajo, Thoracolithiasis—a mobile calcified nodule in the intrathoracic space: radiographic, CT, and MRI findings, Radiat. Med. 20 (3) (2002) 131–133.
[55] T.C. Cheng, A.S. Chou, C.M. Jeng, P.Y. Chang, C.C. Lee, Computed tomography findings of gossypiboma, J. Chin. Med. Assoc. 70 (12) (2007) 565–569.
[56] N. Karabulut, D. Herek, Y. Kiroğlu, CT features of intrathoracic gossypiboma (textiloma), Diagn Interv. Radiol. 17 (2) (2011) 122–124.
[57] R. Madan, B. Trotman-Dickenson, A.R. Hunsaker, Intrathoracic gossypiboma, AJR Am. J. Roentgenol. 189 (2) (2007) W90–W91.
[58] D. Yilmaz Durmaz, B.K. Yilmaz, O. Yildiz, Y. Bas, A rare cause of chronic cough: intrathoracic gossypiboma, Iran. J. Radiol. 11 (2) (2014) e13933.
[59] A. Manzella, P.B. Filho, E. Albuquerque, F. Farias, J. Kaercher, Imaging of gossypibomas: pictorial review, AJR Am. J. Roentgenol. 193 (6 Suppl.) (2009) S94–S101.
[60] E. Marchiori, G. Zanetti, B. Hochhegger, D.M. Machado, Hydatid disease versus textiloma: a diagnostic challenge, Thorax 66 (7) (2011) 635.
[61] I. Ridene, S. Hantous-Zannad, A. Zidi, B. Smati, I. Baccouche, T. Kilani, K. Ben Miled-M'rad, Imaging of thoracic textiloma, Eur. J. Cardiothorac. Surg. 39 (3) (2011) e22–e26.
[62] T. Kokubo, Y. Itai, K. Ohtomo, K. Yoshikawa, M. Iio, Y. Atomi, Retained surgical sponges: CT and US appearance, Radiology 165 (2) (1987) 415–418.
[63] L.F. Nobre, E. Marchiori, F. May, A.D. Carrão Jr., G. Zanetti, D.M. Machado, Thoracic textilomas after myocardial revascularisation: typical CT findings, Br. J. Radiol. 83 (985) (2010) 4–7.
[64] B. Hochhegger, G. Zanetti, T.S. Garcia, E. Marchiori, Retained surgical sponge presenting as a cardiac mass, Eur. J. Cardiothorac. Surg. 41 (5) (2012) e129.
[65] D.M. Machado, G. Zanetti, C.A. Araujo Neto, L.F. Nobre, S. Meirelles Gde, J.L. Pereira E Silva, M.D. Guimarães, D.L. Escuissato, A.S. Souza Jr., B. Hochhegger, E. Marchiori, Thoracic textilomas: CT findings, J. Bras. Pneumol. 40 (5) (2014) 535–542.
[66] T. Suwatanapongched, S. Boonkasem, E. Sathianpitayakul, P. Leelachaikul, Intrathoracic gossypiboma: radiographic and CT findings, Br. J. Radiol. 78 (933) (2005) 851–853.
[67] F. Vayre, P. Richard, J.P. Ollivier, Intrathoracic gossypiboma: magnetic resonance features, Int. J. Cardiol. 70 (2) (1999) 199–200.
[68] R. Gencosmanoglu, R. Inceoglu, An unusual cause of small bowel obstruction: gossypiboma – case report, BMC Surg. 3 (2003 Sep 8) 6.
[69] K.I. Kim, C.W. Kim, M.K. Lee, K.S. Lee, C.K. Park, S.J. Choi, J.G. Kim, Imaging of occupational lung disease, Radiographics 21 (6) (2001) 1371–1391.
[70] H.D. Roach, G.J. Davies, R. Attanoos, M. Crane, H. Adams, S. Phillips, Asbestos: when the dust settles an imaging review of asbestos-related disease, Radiographics 22 (2002). Spec No:S167–S184.
[71] Y.J. Jeong, S. Kim, S.W. Kwak, N.K. Lee, J.W. Lee, K.I. Kim, K.U. Choi, T.Y. Jeon, Neoplastic and nonneoplastic conditions of serosal membrane origin: CT findings, Radiographics 28 (3) (2008) 801–817.
[72] B.M. Haus, P. Stark, S.L. Shofer, W.G. Kuschner, Massive pulmonary pseudotumor, Chest 124 (2) (2003) 758–760.
[73] P. Swathi, S. Chandhar, E. Bhaskar, R. Rajarajan, Pleural effusion masquerading as pseudotumor, Lung India 31 (1) (2014) 86–87.